Published in final edited form as:
Exp Eye Res. 2010 May ; 90(5): . doi:10.1016/j.exer.2010.02.012.

Retinal Vascular Leakage Occurring in GABA *Rho-1* Subunit Deficient Mice

Wei Zheng, **Xiaoping Zhao**, **Jie Wang**, and **Luo Lu**[*]
Division of Molecular Medicine, Department of Medicine, David Geffen School of Medicine, University of California Los Angeles, Torrance, CA 90502

Abstract

Recent studies demonstrate that GABAergic activity elicits relaxation of retinal arterioles leading to an increase in blood flow. It has also been found that GABAnergic activity in the retina of mice with diabetic retinopathy is suppressed. In this study, we provide further evidence that lack of GABAergic activity significantly alters vasculature development as well as the hypoxia-induced angiogenic response. Using $GABA_C$ receptor ρ_1 subunit knockout mice (*rho-1*$^{-/-}$), our results demonstrate that in hypoxia-induced retinas a severe vascular leakage occurred in 2 week-old *rho-1*$^{-/-}$ mice compared with their wildtype counterparts. In addition, our results also showed that all of the *rho-1*$^{-/-}$ mice developed significant retinal vascular leakages by 48 weeks of age. Microarray and real time PCR experiments revealed a unique angiogenesis-related gene expression pattern. This suggests that retinal vascular disorders of *rho-1*$^{-/-}$ mice results from significant up-regulation of angiogenic genes and concomitant down-regulation of anti-angiogenic genes. The study results are consistent with the pathological changes of the retinal vascular leakage seen in diabetic retinopathy. Our data indicate that the $GABA_C$ ρ_1 subunit plays a role in maintaining both homeostasis and balance of retinal neurotransmitter function. Knockout of the retinal $GABA_C$ ρ_1-subunit leads to changes in vascular permeability similar to the pathological changes induced by retinal hypoxic conditions.

Keywords

Gene expression; angiogenesis; retinopathy; microarray; transgenic animal

Introduction

GABA is the major inhibitory neurotransmitter in the vertebrate central nervous system (CNS). The $GABA_C$ receptor is predominantly found in retina tissue. This receptor forms homo-oligomeric and hetero-oligomeric Cl^- channels through combinations of ρ_1 and ρ_2 subunits(Cutting et al., 1991; Wang et al., 1994). Homo-oligomeric $GABA_C$ receptor/channels formed by ρ_1 subunits is involved in mediating lateral inhibition and local gain control circuitry (Dong et al., 1998; Feigenspan et al., 1998; Lukasiewicz et al., 1994). A number of studies suggest that the diabetic state affects the retina by causing an increase in the concentration of glutamate as well as a decrease in efficacy of $GABA_C$ receptor gene

[*]Address correspondence to: Luo Lu, M.D., Ph.D., Division of Molecular Medicine, UCLA School of Medicine, Harbor-UCLA Medical Center, 1124 W. Carson Street, C-2, Torrance, CA 90502, Tel. 310 787-6853, Fax. 310 222-3781, lluou@ucla.edu.

transcription (Ambati et al., 1997; Kowluru et al., 2001; Lieth et al., 1998) (Ramsey et al., 2007). In cases of diabetic retinopathy, the decreased $GABA_C$ receptor expression leads to a compensatory increase in GABA neurotransmitter and glutamate concentration in the vitreous (Barber, 2003; Ng et al., 2004; Puro, 2002; Santiago et al., 2006; Ward et al., 2005). Interestingly, GABA receptors can elicit a relaxing influence on isolated retinal arterioles. This suggests that the inhibitory activity of the GABA receptor can regulate the arteriolar tone (Holmgaard et al., 2008).

Histopathological findings in proliferative diabetic retinopathy (DR) and other ocular disorders show vascular leakages. The subsequent retinal edema is often associated with retinal hypoxia. This cascade of events is known to induce vascular endothelial growth factor (VEGF) production (Aiello et al., 1998; Antonetti et al., 1998; Ciulla et al., 1998; Klein, 1996). It has been suggested that the increase in GABA concentration seen in hypoxic conditions is a self-protective mechanism to counteract the glutamate-induced excitotoxicity. Vascular leakage caused by the breakdown of the blood-retinal barrier is associated with the development of DR, increased oxidative stress, enhanced VEGF production, elevated endothelin and nitric oxide (NO) levels, increased polyol formation, increased protein kinase C (PKC) activity, and the formation of advanced glycation end (AGE) products. Each proposed biochemical mechanism for developing DR has been exploited for possible treatments. Notably, several pro-angiogenic growth factors including VEGF, IGF-1, and PDGF, as well as anti-angiogenic factors including PEDF, TIMP and TGF-β (note: the effect of TGF-β on angiogenesis has not been completely defined yet), have been found to be involved in the neovascularization process in the retina (Das et al., 2003). Currently, most studies have been focused on VEGF; in animal models and patients with DR, VEGF has been shown to be adequate for increasing both vascular proliferation and permeability (Aiello et al., 1994; Ambati et al., 1997; Sone et al., 1997). However, the pathogenesis of retinal NV in DR patients is still uncertain. In the present study, we provide experimental data to support the role of the GABA inhibitory neuropathway in protection of the retinal integrity and normal function. In the retina of $GABA_C$ receptor knockout *rho-1*$^{-/-}$ mice, we found that there were alterations in angiogenesis-related gene expression very similar to the changes observed in diabetic retinopathy. Our results show that expression of the angiogenic genes was increased; and that expression of anti-angiogenic genes was decreased in the retina of the *rho-1*$^{-/-}$ mice. As a result of these changes, it developed abnormal vasculature, neovascularization and vascular leakages in the retina of GABA *rho-1* subunit deficient mice.

Materials and Methods

Animals

The experiments were performed using wild-type C57BL/6J (*rho-1*$^{+/+}$), and $GABA_C$ receptor ρ_1 subunit knockout (*rho-1*$^{-/-}$) mice back-bred into C57BL/6J genetic background. C57BL/6J mice with targeted disruption of the $GABA_C$ receptor ρ_1 subunit (*rho-1*$^{-/-}$) were generated as described in a previous publication.(Zheng et al., 2003) The genotypes of those animals were identified by Southern analysis. Both *rho-1*$^{+/+}$ and *rho-1*$^{-/-}$ mice used in comparative studies, gene microarray and real time RT-PCR experiments were from the same litter, and mixed-housed to ensure the best comparability. All animals were treated in accordance with the ARVO Statement for the Use of Animals in Ophthalmic and Vision Research, using protocols approved and monitored by the Animal Care Committee of Harbor-UCLA Medical Center, David Geffen School of Medicine at UCLA. A hyper-oxygen stimulation model was used to induce hypoxic response in mice in that newborn mice were kept in 75% oxygen for 5 days (P7–P12) and returned to room air. Abnormal development of retinal vascularization was detected in five days (P17).

Capillary Permeability Measurement

Permeability of retinal vascular system was measured *in vivo* with an approach adapted from previous studies in rats.(Antonetti et al., 1998) Bovine serum albumin conjugated with FITC (BSA-FITC, 100 μg/g; Sigma-Aldrich, St. Louis, MO) were injected into the tail vein of mice that were anesthetized with pentobarbital (100 mg/kg). Thirty minutes later, the mice were rapidly decapitated, and both eyes were enucleated and immersed in ice-cold 4% paraformaldehyde for 1 h. After fixation, eyes were flash-frozen in OCT (Tissue-Tek, Torrance, CA) by rapid immersion of tissues in 2-methylbutane cooled with dry ice. Serial cryostat sections (10 μm) of the eyes were mounted in aqueous medium (Polysciences, Warrington, PA). The relative fluorescence was measured by a computer-controlled fluorescence microscope with an image analysis program in multiple regions of sections from wildtype and *rho-1*$^{-/-}$ mice.

Determination of retinal vasculature and neovascularization

The morphology and distribution of retinal blood vessels were analyzed in retinal frozen sections (10 μm in thickness) labeled with biotinylated Griffonia simplicifolia isolectin B4 (Vector Laboratories, Burlingame, CA) and fluorescein-conjugated Avidin D (Dako, Glostrup, Denmark). Serial sections were cut through the entire extent of the eye. The entire eye was sampled at 100 μm apart, which provided 12 sections per eye for analysis. Sections were histochemically stained with biotinylated *Griffonia simplicifolia* lectin B4 that selectively binds to vascular cells. Slides were incubated in 4% paraformaldehyde for 30 min, washed with 50 mM Tris buffer (TB; pH 7.4), incubated in methanol-H_2O_2 for 10 min at 4°C, washed with 50 mM TB, and incubated for additional 30 min in 10% normal swine serum. Slides were rinsed with 50 mM TB and incubated 2 h at 37°C with 1:20 GSA, rinsed again with 50 mM TB, and incubated with undiluted fluorescein-conjugated Avidin D for 30 min at 22°C. After a 10-min wash with 50 mM TB (pH 7.6), the slides were covered with fluorescent mounting medium. Densities of the retinal blood vessels were counted and statistically analyzed.

Microarray and real time RT-PCR

Six littermate mice at 48 week-old were sacrificed by cervical dislocation. Eyeballs were excised and the retinal tissues with retinal pigment epithelial (RPE) cell layer were isolated. Tissues were immediately immersed in liquid nitrogen and then placed in the −80 °C freezer. For mRNA isolation, fresh frozen tissues were homogenized in TRIZOL (GIBCO). Total RNAs were isolated with RNeasy spin columns (Qiagen). An Oligotex mRNA purification Kit (Qiagen) was used to purified mRNA and mRNAs were quantified by readings of OD 260. The OD 260/280 ratio was normally around 2.0. The quality of each RNA sample was analyzed with RNA 600 Nano LabChip using the Agilent 2100 Bioanalyzer (Agilent Technologies). Each mRNA sample (2.5 μg) was used to amplify and synthesize biotin-labeled cRNA with MessageAmp kit (Ambion). Biotin-labeled cRNA samples were fragmented at 94 °C for 35 min with fragmentation buffer. Fragmented cRNA (10 μg) was mixed with 3.3 μl of control oligonucleotide B2 (3 nM), 10 μl of 20X eukaryotic hybridization controls (*bioB, bioC, bioD, cre*), 2 μl of herring sperm DNA (10 mg/ml), 2 μl of acetylated BSA (50 mg/ml), 100 μl of 2x hybridization buffer and ddH_2O to make 200 μl of hybridization cocktail. Probe arrays were performed in 1X hybridization buffer at 45 °C for 10 min in a hybridization cocktail pre-heated to 99 °C for 5 min and the Affymetrix Murine Genome Arrays U74Av2 were filled with the hybridization cocktail and hybridized for 16 h in 45 °C GeneChip Hybridization Oven 640 rotating at 60 rpm. The hybridized probe arrays were washed and stained with standard Affymetrix washing and staining procedure on GeneChip Fluidics Station 400 using an antibody amplification protocol for eukaryotic targets. Probe arrays were scanned with Agilent GeneArray Scanner

after the wash protocols were complete. Gene expression profile for each individual mouse was obtained. The data were analyzed using GeneChip Operating Software (Affymetrix) and GeneSping 6.1 (Silicon Genetics).

SYBR Green Quantitative Real-time PCR was performed on ABI PRISM 7700 Sequence Detection System (Applied Biosystmes). The aliquots of the same total RNA samples were subjected to SYBR green quantitative real-time PCR analysis. After treatment of DNase I, each of the RNA samples was reverse-transcribed into cDNA using 2.5 μM of random hexamers and 2 units of MultiScrib Reverse Transcriptase (Applied Biosystems). The cDNA (100 ng) was used as amplification template in SYBR green real-time PCR assays using QuantiTect SYBR green PCR kit (Qiagen). The mouse GAPDH gene was used as endogenous reference in the real-time PCR for relative quantization assay with its specific primers (forward: 5'-ATGACTCCACTCACGGCAAATT-3', reverse: 5'-TCCCATTCTCGGCCTTGACTGT-3'). The target genes for relative quantization and their gene-specific primers were: PEDF, forward primer: 5'-AGATTACTGGCAAACCCGTGAA-3', reverse primer: 5'-GAAAGCAGCCCTGTGTTCCA-3'; IGF-1, forward primer: 5'-TCCCACGGAGCAGAAAATG-3', reverse primer: 5'-GCTCAAGCAGCAAAGGATCCT-3'; VEGF-1, forward primer: 5'-GGCGAGGCAGCTTGAGTTAA-3', reverse primer: 5'-CTTGGCTTGTCACATCTGCAA-3'; VEGFR-2, forward primer: 5'-TGGAAGGTTTGCGTGCTCTT-3', reverse primer: 5'-CCACAGGGAACTCGCCTGTA-3'. A validation experiment was performed to demonstrate that the amplification efficiencies of target and reference (GAPDH) were approximately equal with the absolute value of the slope of log input amount vs. ΔC_T (threshold cycle difference) < 0.1. After the validation experiment, all target genes were relatively quantified (*rho1*$^{-/-}$ vs. *rho1*$^{+/+}$) with comparative C_T method. The amount of target (target gene in *rho1*$^{-/-}$) normalized to an endogenous reference (GAPDH) and relative to a calibrator (target gene in *rho1*$^{+/+}$), was given by: fold change (*rho1*$^{-/-}$/*rho1*$^{+/+}$) = $2^{-\Delta\Delta CT}$, where $\Delta\Delta C_T = \Delta C_{T,\,q} - \Delta C_{T,ca}$ ($\Delta C_T = C_{T,target} - C_{T,reference}$).

Immunohistochemistry and Nissl stain

Adult mice (*rho1*$^{-/-}$ and *rho1*$^{+/+}$) were overdosed with 5% sodium pentobarbital, and then transcardially perfused with 4% paraformaldehyde in phosphate buffered saline (PBS) for 15 min. Eyeballs were excised and placed overnight in 10%, 20% and 30% sucrose PBS solution series for cryoprotection. The retinal tissue was dissected out and embedded in OCT® compound (Fisher Scientific). The tissue sections (10-20 μm) were cut on a cryostat (Zeiss), and thaw-mounted onto slides, air-dried and stored at −80 °C. For immunohistochemistry experiments, the sections were encircled with hydrophobic resin (PAP Pen) and incubated at 22 °C for 1 h in PBS with 10% goat serum, 0.5% Triton X-100 and 1% BSA to block non-specific antibody binding. Rabbit ρ-subunit-specific antiserum was applied to the sections at 1:100 dilution at 4°C overnight (Ekema et al., 2001). The sections were incubated with Alexa488-goat anti-rabbit IgG (Molecular Probes) 1:250 in PBS at 22 °C for 2 h. NeuroTrace™ red fluorescence Nissl stain (Molecular Probes) 1:100 solution in PBS with 0.1% Triton X-100 was applied to the sections for 20 min. The sections were washed for 10 min in PBS containing 0.1% Triton X-100, followed by incubation in PBS for 1 h. The slides were viewed under Leica microscope and the images were captured by Leica TCS SP2 laser-scanning confocal microscope with proper filter sets (Leica, Germany).

Results

Previous reports suggest that the GABA receptor/channel ρ_1 subunit is primarily located in the inner and outer plexiform layers, and cell bodies of bipolar cells.(Enz et al., 1996; Koulen et al., 1998; Koulen et al., 1997). Our results showed strong immunoreactivities of the ρ_1 subunit in the inner plexiform layer (IPL) and weaker immunoreactivities in the outer plexiform layer (OPL) (Fig. 1A), consistent findings with previous reports. The ρ_1 subunit was completely deficient in the retina of *rho-1*$^{-/-}$ mice although these mice had normally developed retinal structures. In the retina of 8 week-old *rho-1*$^{-/-}$ mice, immunostaining and confocal microscopy results revealed that $GABA_C$ ρ_1 subunits were absent, Furthermore, there were no changes in neuronal distribution or Nissl stained structures (Fig. 1B, upper panels represent wildtype retinas and lower panels represent *rho-1*$^{-/-}$ retinas).

The effect of knocking out the $GABA_C$ ρ_1 subunit on retinal vasculature development was studied in normaxic and hypoxic conditions. Hypoxia-induced alterations of the retinal vasculature were evaluated by vascular distribution and vessel densitiy measurementses. Frozen sections of retinas obtained from 17 day-old wildtype and *rho-1*$^{-/-}$ mice were stained with endothelial cell–specific lectin Griffonia simplicifolia using peroxidase-antiperoxidase technique (Fig. 2A). There were significantly fewer positive staining endothelial cells in retinal sections of *rho-1*$^{-/-}$ mice compared with retinal sections from wildtype mice. Also, in *rho-1*$^{-/-}$ mice, some areas showed clumps of endothelial cells. Hypoxic conditions were induced by exposure of 7 day-old mice (P7) in an animal chamber containing 75% oxygen for 5 days followed by placing the mice in normal room air for an additional 5 days (P17). Hypoxia-induced retinal neovascularization was analyzed in both wildtype and *rho-1*$^{-/-}$ mice. Endothelial cell numbers from wildtype and *rho-1*$^{-/-}$ mice were significantly increased in retinal samples from 112±2.6 to 156±8.0 per section, and from 81±2.3 to 172±8.2 per section respectively (Fig. 2B). These results demonstrated changes in morphology and distribution of the retinal vasculature. In addition, statistical analysis of hypoxia-induced and newly formed vessels in the retina revealed that there was a significant increase in neovascularization in response to hypoxic stimulation in *rho-1*$^{-/-}$ mice compared with wildtype mice.

To investigate the effect of a $GABA_C$ ρ_1 subunit knockout on retinal neovascularization, we measured vascular permeability and assessed retinal edema. We performed a series of FITC-labeled albumin perfusion experiments to detect leakages in the retinal vascular system of 48 week-old wildtype and *rho-1*$^{-/-}$ mice side by side. The retinal vascular leakages of wildtype and *rho-1*$^{-/-}$ mice were examined by flat/whole-mounted retinal microscopy (Fig. 3A, upper panels a&b). At magnified views, there were clearly visible signs of vascular leakages in the retina of *rho-1*$^{-/-}$ mice compared with the retina of wildtype mice (Fig. 3A, lower panel c&d). Further analysis of retinal vascular leakages was performed in retinal slides of wildtype and *rho-1*$^{-/-}$ mice. We found that there were massive vascular leakages in the retina slides of 48 week-old *rho-1*$^{-/-}$ mice (Fig. 3B). FITC florescent intensities in retinal slides in areas with a standardized size were measured for wildtype (22±0.2%) and *rho-1*$^{-/-}$ (68±06%) mice using a scan program. There were increases in fluorescent intensities of more than 3.0 folds in retinal slides of *rho-1*$^{-/-}$ mice compared with wildtype retinal slides. This indicates that there were significantly increased leakages of the vasculature (Fig. 3B, right panel).

Microarray analysis was performed to detect alterations of global gene expression profiling in retinas of *rho-1*$^{-/-}$ mice and their wildtype (*rho-1*$^{+/+}$) littermates at 48 weeks-of-age. Total RNA from the retina and retinal pigment epithelial (RPE) cells was extracted from six littermates of *rho-1*$^{-/-}$ and *rho-1*$^{+/+}$ mice. The gene expression profile for each individual mouse was obtained using the Affymetrix MG_U74Av2 array. The data was analyzed using GeneSping 6.1 according to functional gene ontology. Unique and interesting patterns of

gene expression modulations were discovered in *rho-1*$^{-/-}$ mice. Most notable was that the shift in balance between retinal angiogenic and anti-angiogenic gene expression patterns now favored angiogenesis. Expression of VEGF was up-regulated 2.3 fold and its receptor KDR (VEGFR-2) increased 1.9 fold. Other angiogenic factors, such as IGF-1 and PDGF, were also increased 1.8 fold and 1.5 fold, respectively (Fig. 4A). In contrast, PEDF, the anti-angiogenic factor, was down-regulated 1.79 fold (Fig 4B). Other potentially anti-angiogenic factors, including TIMP, TGF-β, TSP-1 and FLT-1, were also found to be significantly down-regulated. This altered pattern of gene expression favoring angiogenesis is strikingly similar to the pattern observed in retinal neovascularization. Expression of hypoxia inducible factor, HIF-1α, was markedly increased in *rho-1*$^{-/-}$ mouse retinas, indicating pre-existing hypoxic conditions in the retina (Fig. 2A). Results from microarray experiments were further verified by SYBR-Green-I based real-time and quantitative PCR experiments (Fig. 5). We found that in the retina of *rho-1*$^{-/-}$ mice, expressions of VEGF, IGF-1 and KDR were increased by 2.65, 1.8 and 2.2 folds, respectively. However, the anti-angiogenic gene PEDF was markedly decreased by 0.58 fold. Gene profiling data demonstrated for the first time that the knockout of the $GABA_C$ ρ_1 subunit in the retina induced up-regulation of angiogenic gene expression and down-regulation of anti-angiogenic gene expression. This gene expression profile in *rho-1*$^{-/-}$ mice resulted in retinal vasculature disorders.

Discussion

Retinal edema is an indicator of developing vascular pathology in diabetic patients; it is characterized by abnormal development of retinal neovascularization leading to by a breakdown of the blood–retina barrier (Lieth et al., 2000a). Using homologous recombination techniques, a $GABA_C$ receptor ρ_1 subunit-knockout mouse (*rho-1*$^{-/-}$) was engineered. These mice are more suceptable to hypoxia-induced retinal edema the associated retinal vasculature aberrations. These aberrations are similar to those found in the retina of 36 week-old $Ins2^{Akita}$ diabetic mice.(Barber et al., 2005) Retinal neovascularization in $Ins2^{Akita}$ diabetic mice are similar and compatible to pathological changes found in the earlier phase of diabetic retinopathy.(Amin et al., 1997; Barber et al., 2005; Lutty et al., 1996)

Significant changes in gene expression patterns were identified by microarray experiments. This indicats that there were alterations in angiogenesis-related gene expressions in the retina of *rho-1*$^{-/-}$ mice. It has been suggested that pathological angiogenesis resulting from altered expression levels of VEGF, FGF2, angiopoietins, PEDF, nitric oxide and TSP-1 are major factors in retinal edema development. However, the precise molecular mechanism has not been elucidated yet.(Abecasis et al., 2004; Ambati et al., 2003) Our data form *rho-1*$^{-/-}$ mice demonstrates retinal pathological changes due to hyper-expression of angiogenic stimulators (VEGF, IGF-1, PDGF) and decreased expression of angiogenic inhibitors (PEDF, TGF-β). These changes contribute to the increased retinal vascular permeability which characterises the retinal edema in DR. The abnormal retinal vasculature were confirmed by measuring increases in vascular leakages in the retina (Fig. 3). In addition, studies of altered retinal gene expression pattern resulting from loss of function of $GABA_C$ receptor ρ_1 subunit activity are critical for understanding molecular mechanisms underlying various diseases such as diabetic retinopathy.

We found that retinal edema occurred only in mature *rho-1*$^{-/-}$ mice. This suggests that $GABA_C$ receptor deficiency may not be sufficient to initiate pathological changes of retinopathy in younger ages of the transgenic mice. Genetic predisposition due to lacking $GABA_C$ receptor activity in *rho-1*$^{-/-}$ mice could result in oxidative stress to retinal cells leading to abnormal expression of genes that are related to pathological angiogenesis in the retina. However, we believe from our results that $GABA_C$ receptor contributes significantly

to the protection of retinal tissues from excitotoxicity that can lead to hypoxic condition in the retina. Tolerance of retinal tissues to hypoxic stress in young *rho-1*$^{-/-}$ mice is significantly altered from wildtype mice by showing a significant increase in hypoxia-induced neovascularization (Fig. 2). The result from the retina of the younger mice is consistent to the observation that neovascularization and vascular leakages occurred in the retinas of mature *rho-1*$^{-/-}$ mice, which further supports the notion that there is hypoxia in the retina of *rho-1*$^{-/-}$ mice.

Accumulative evidence suggests that the breakdown of the blood-retina barrier and subsequent retinal edema are results of developing vascular pathogenesis, such as neovascularization, in response to hypoxic conditions and to excitotoxicity induced by excitatory neurotransmitter glutamate in the retina. It has been suggested that the increase in GABA concentration is a protective mechanism in the retina; it counteracts glutamate-induced excitotoxicity. In fact, significant increase in GABA concentration in the vitreous is found in diabetic retinas in that there is an increased glutamate concentration.(Honda et al., 1998; Kowluru et al., 2001; Lieth et al., 1998; Lieth et al., 2000b; Santiago et al., 2006; Ward et al., 2005) Through our data, we were unable to draw a conclusion as to whether there was a significant change in glutamate receptors in $GABA_C$ receptor *rho-1-/-* mice. However, it is likely that $GABA_C$ receptor activity increases in response to elevated GABA release in the retina. This serves to protect retinal neurons from excitotoxicity and to control the hypoxic conditions caused by hyperglycemia and excess of glutamate. Naturally, $GABA_C$ receptor *rho-1*$^{-/-}$ mice, lacking such protective mechanism, are more susceptible to developing retinal edema.

Acknowledgments

This study is supported by NIH grants EY012757 to L.L.

References

Abecasis GR, Yashar BM, Zhao Y, Ghiasvand NM, Zareparsi S, Branham KE, Reddick AC, Trager EH, Yoshida S, Bahling J, Filippova E, Elner S, Johnson MW, Vine AK, Sieving PA, Jacobson SG, Richards JE, Swaroop A. Age-related macular degeneration: a high-resolution genome scan for susceptibility loci in a population enriched for late-stage disease. Am J Hum Genet. 2004; 74:482–494. [PubMed: 14968411]

Aiello LP, Avery RL, Arrigg PG, Keyt BA, Jampel HD, Shah ST, Pasquale LR, Thieme H, Iwamoto MA, Park JE, et al. Vascular endothelial growth factor in ocular fluid of patients with diabetic retinopathy and other retinal disorders. N Engl J Med. 1994; 331:1480–1487. [PubMed: 7526212]

Aiello LP, Gardner TW, King GL, Blankenship G, Cavallerano JD, Ferris FL 3rd, Klein R. Diabetic retinopathy. Diabetes Care. 1998; 21:143–156. [PubMed: 9538986]

Ambati J, Ambati BK, Yoo SH, Ianchulev S, Adamis AP. Age-related macular degeneration: etiology, pathogenesis, and therapeutic strategies. Surv Ophthalmol. 2003; 48:257–293. [PubMed: 12745003]

Ambati J, Chalam KV, Chawla DK, D'Angio CT, Guillet EG, Rose SJ, Vanderlinde RE, Ambati BK. Elevated gamma-aminobutyric acid, glutamate, and vascular endothelial growth factor levels in the vitreous of patients with proliferative diabetic retinopathy. Arch Ophthalmol. 1997; 115:1161–1166. [PubMed: 9298058]

Amin RH, Frank RN, Kennedy A, Eliott D, Puklin JE, Abrams GW. Vascular endothelial growth factor is present in glial cells of the retina and optic nerve of human subjects with nonproliferative diabetic retinopathy. Invest Ophthalmol Vis Sci. 1997; 38:36–47. [PubMed: 9008628]

Antonetti DA, Barber AJ, Khin S, Lieth E, Tarbell JM, Gardner TW. Vascular permeability in experimental diabetes is associated with reduced endothelial occludin content: vascular endothelial growth factor decreases occludin in retinal endothelial cells. Penn State Retina Research Group. Diabetes. 1998; 47:1953–1959. [PubMed: 9836530]

Barber AJ. A new view of diabetic retinopathy: a neurodegenerative disease of the eye. Prog Neuropsychopharmacol Biol Psychiatry. 2003; 27:283–290. [PubMed: 12657367]

Barber AJ, Antonetti DA, Kern TS, Reiter CE, Soans RS, Krady JK, Levison SW, Gardner TW, Bronson SK. The Ins2Akita mouse as a model of early retinal complications in diabetes. Invest Ophthalmol Vis Sci. 2005; 46:2210–2218. [PubMed: 15914643]

Ciulla TA, Danis RP, Harris A. Age-related macular degeneration: a review of experimental treatments. Surv Ophthalmol. 1998; 43:134–146. [PubMed: 9763138]

Cutting GR, Lu L, O'Hara BF, Kasch LM, Montrose-Rafizadeh C, Donovan DM, Shimada S, Antonarakis SE, Guggino WB, Uhl GR, et al. Cloning of the gamma-aminobutyric acid (GABA) rho 1 cDNA: a GABA receptor subunit highly expressed in the retina. Proc Natl Acad Sci U S A. 1991; 88:2673–2677. [PubMed: 1849271]

Das A, McGuire PG. Retinal and choroidal angiogenesis: pathophysiology and strategies for inhibition. Prog Retin Eye Res. 2003; 22:721–748. [PubMed: 14575722]

Dong CJ, Werblin FS. Temporal contrast enhancement via GABAC feedback at bipolar terminals in the tiger salamander retina. J Neurophysiol. 1998; 79:2171–2180. [PubMed: 9535976]

Ekema GM, Zheng W, Wang L, Lu L. Modulation of recombinant GABA receptor/channel subunits by domain- specific antibodies in Xenopus oocytes. J Membr Biol. 2001; 183:205–213. [PubMed: 11696862]

Enz R, Brandstatter JH, Wassle H, Bormann J. Immunocytochemical localization of the GABAc receptor rho subunits in the mammalian retina. J Neurosci. 1996; 16:4479–4490. [PubMed: 8699258]

Feigenspan A, Bormann J. GABA-gated Cl- channels in the rat retina. Prog Retin Eye Res. 1998; 17:99–126. [PubMed: 9537798]

Holmgaard K, Aalkjaer C, Lambert JD, Hessellund A, Bek T. The relaxing effect of perivascular tissue on porcine retinal arterioles in vitro is mimicked by N-methyl-D-aspartate and is blocked by prostaglandin synthesis inhibition. Acta Ophthalmol. 2008; 86:26–33. [PubMed: 17944976]

Honda M, Inoue M, Okada Y, Yamamoto M. Alteration of the GABAergic neuronal system of the retina and superior colliculus in streptozotocin-induced diabetic rat. Kobe J Med Sci. 1998; 44:1–8. [PubMed: 9846053]

Klein R. Diabetic retinopathy. Annu Rev Public Health. 1996; 17:137–158. [PubMed: 8724221]

Koulen P, Brandstatter JH, Enz R, Bormann J, Wassle H. Synaptic clustering of GABA(C) receptor rho-subunits in the rat retina. Eur J Neurosci. 1998; 10:115–127. [PubMed: 9753119]

Koulen P, Brandstatter JH, Kroger S, Enz R, Bormann J, Wassle H. Immunocytochemical localization of the GABA(C) receptor rho subunits in the cat, goldfish, and chicken retina. J Comp Neurol. 1997; 380:520–532. [PubMed: 9087530]

Kowluru RA, Engerman RL, Case GL, Kern TS. Retinal glutamate in diabetes and effect of antioxidants. Neurochem Int. 2001; 38:385–390. [PubMed: 11222918]

Lieth E, Barber AJ, Xu B, Dice C, Ratz MJ, Tanase D, Strother JM. Glial reactivity and impaired glutamate metabolism in short-term experimental diabetic retinopathy. Penn State Retina Research Group. Diabetes. 1998; 47:815–820. [PubMed: 9588455]

Lieth E, Gardner TW, Barber AJ, Antonetti DA. Retinal neurodegeneration: early pathology in diabetes. Clin Experiment Ophthalmol. 2000a; 28:3–8. [PubMed: 11345341]

Lieth E, LaNoue KF, Antonetti DA, Ratz M. Diabetes reduces glutamate oxidation and glutamine synthesis in the retina. The Penn State Retina Research Group. Exp Eye Res. 2000b; 70:723–730. [PubMed: 10843776]

Lukasiewicz PD, Werblin FS. A novel GABA receptor modulates synaptic transmission from bipolar to ganglion and amacrine cells in the tiger salamander retina. J Neurosci. 1994; 14:1213–1223. [PubMed: 7907138]

Lutty GA, McLeod DS, Merges C, Diggs A, Plouet J. Localization of vascular endothelial growth factor in human retina and choroid. Arch Ophthalmol. 1996; 114:971–977. [PubMed: 8694733]

Ng YK, Zeng XX, Ling EA. Expression of glutamate receptors and calcium-binding proteins in the retina of streptozotocin-induced diabetic rats. Brain Res. 2004; 1018:66–72. [PubMed: 15262206]

Puro DG. Diabetes-induced dysfunction of retinal Muller cells. Trans Am Ophthalmol Soc. 2002; 100:339–352. [PubMed: 12545700]

Ramsey DJ, Ripps H, Qian H. Streptozotocin-induced diabetes modulates GABA receptor activity of rat retinal neurons. Exp Eye Res. 2007; 85:413–422. [PubMed: 17662714]

Santiago AR, Pereira TS, Garrido MJ, Cristovao AJ, Santos PF, Ambrosio AF. High glucose and diabetes increase the release of [3H]-D-aspartate in retinal cell cultures and in rat retinas. Neurochem Int. 2006; 48:453–458. [PubMed: 16513217]

Sone H, Kawakami Y, Okuda Y, Sekine Y, Honmura S, Matsuo K, Segawa T, Suzuki H, Yamashita K. Ocular vascular endothelial growth factor levels in diabetic rats are elevated before observable retinal proliferative changes. Diabetologia. 1997; 40:726–730. [PubMed: 9222654]

Wang TL, Guggino WB, Cutting GR. A novel gamma-aminobutyric acid receptor subunit (rho 2) cloned from human retina forms bicuculline-insensitive homooligomeric receptors in Xenopus oocytes. J Neurosci. 1994; 14:6524–6531. [PubMed: 7965056]

Ward MM, Jobling AI, Kalloniatis M, Fletcher EL. Glutamate uptake in retinal glial cells during diabetes. Diabetologia. 2005; 48:351–360. [PubMed: 15688208]

Zheng W, Xie W, Zhang J, Strong JA, Wang L, Yu L, Xu M, Lu L. Function of gamma-aminobutyric acid receptor/channel rho 1 subunits in spinal cord. J Biol Chem. 2003; 278:48321–48329. [PubMed: 12970343]

Abbreviations

DR	Diabetic Retinopathy
FGF	Fibroblast Growth Factor
FITC	Fluorescein Isothiocyanate
IGF	Insulin-like Growth Factor
NV	Neovascularization
NO	Nitric Oxide
PEDF	Pigment Epithelium-Derived Factor
PDGF	Platelet-Derived Growth Factor
TGF	Transforming Growth Factor
VEGF	Vascular Endothelial Growth Factor

A

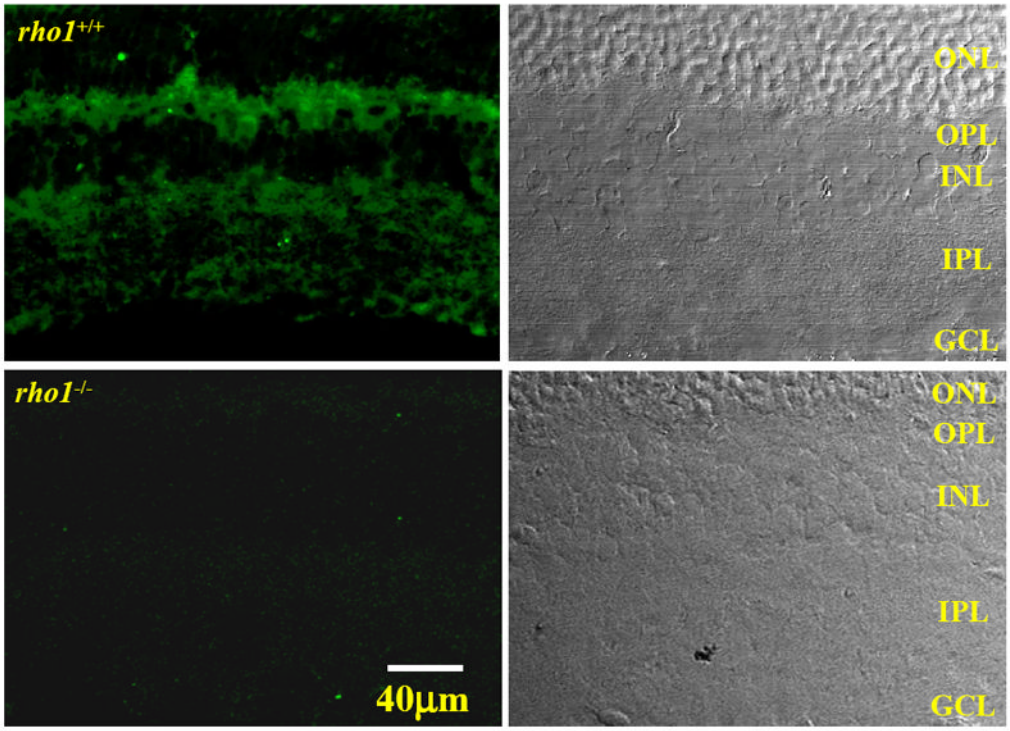

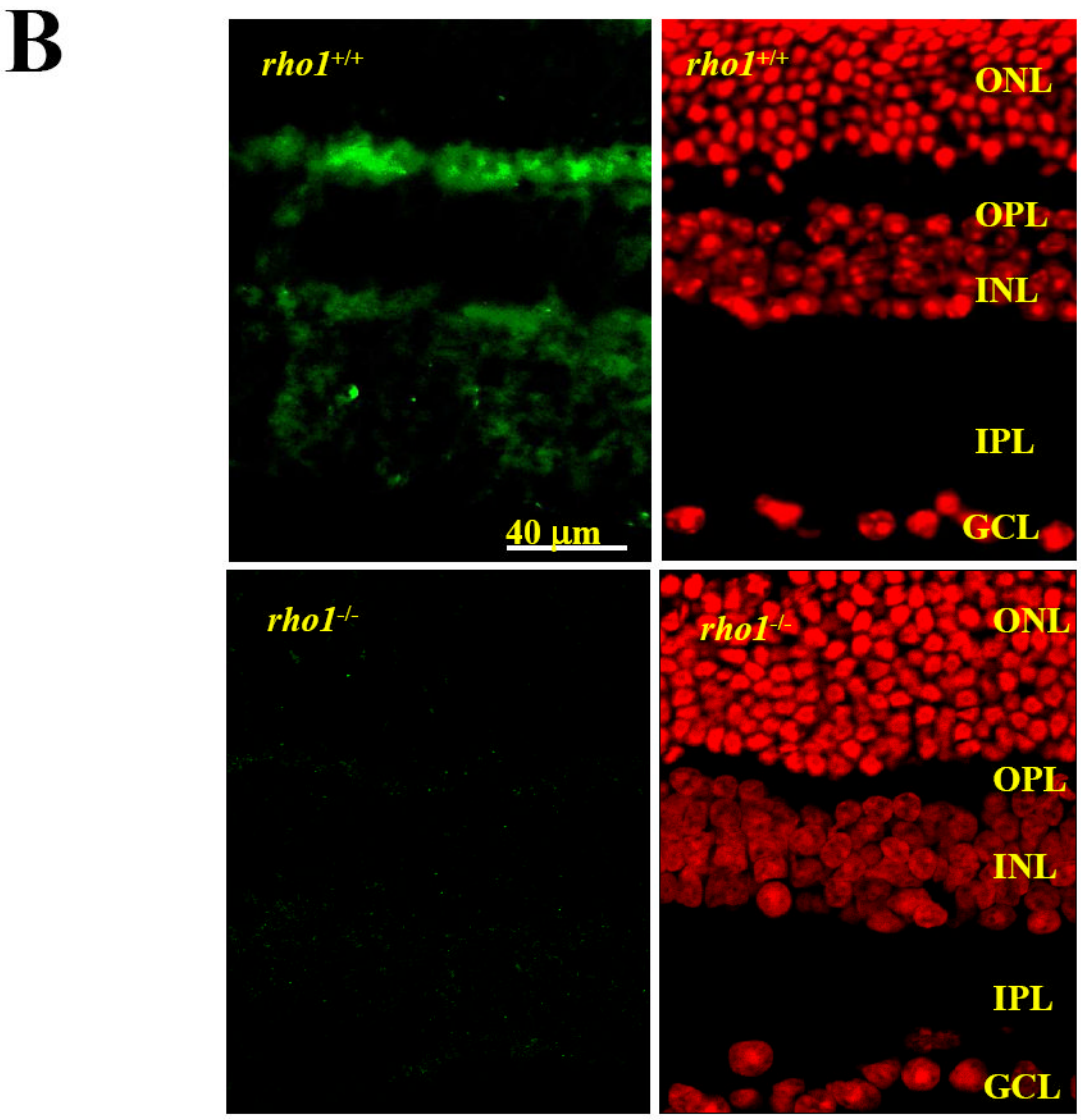

Figure 1.

Expression of $GABA_C$ receptor ρ1 subunit in wildtype (*rho-1*$^{+/+}$) and *rho-1*$^{-/-}$ mice. **(A)** Immunohistochemistry of *rho-1*$^{+/+}$ and *rho-1*$^{-/-}$ mouse retinas using rabbit anti-$GABA_C$ receptor antibodies. **(B)** Normal development of the retina from wildtype and *rho-1*$^{-/-}$ mice. Retinal slides obtained from 8 week-old wildtype and *rho-1*$^{-/-}$ mice were subjected to immunostaining with anti-$GABA_C$ receptor antibody (left panels), and the Nissl stain (right panels). The images were captured using the laser confocal scanning microscopy (Leica). Scale bar denotes 40 μm.

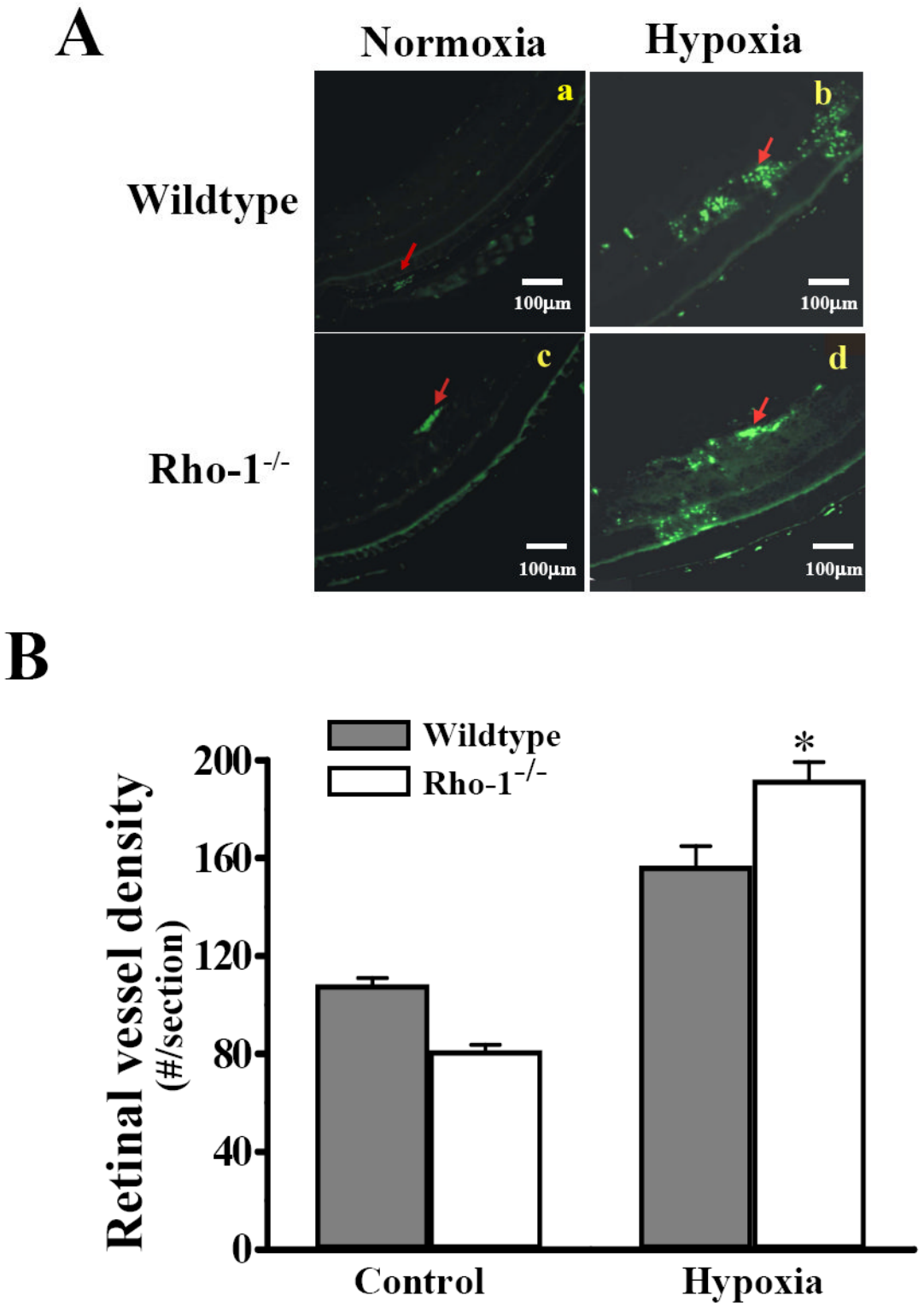

Figure 2.

Development of retinal vasculature and hypoxia-induced neovascularization. **(A)** Assessment of retinal blood vessels and hypoxia-induced retinal neovascularization in wildtype and *rho-1*$^{-/-}$ mice. Retinal blood vessels and hypoxia-induced neovascularization of

17 day-old wildtype mice (a & b) were stained to compare with the *rho-1*$^{-/-}$ retina (c &d). Arrows indicate positively immunostained endothelial cells. **(B)** Quantification of the total area of endothelial cell staining in retinal sections of wild-type and *rho-1*$^{-/-}$ mice. Retinal frozen sections were histochemically stained with endothelial cell-selective lectin *Griffonia simplicifolia* using the peroxidase-antiperoxidase technique. Symbol (*) indicates statistical significance ($n = 8$, $p < 0.01$).

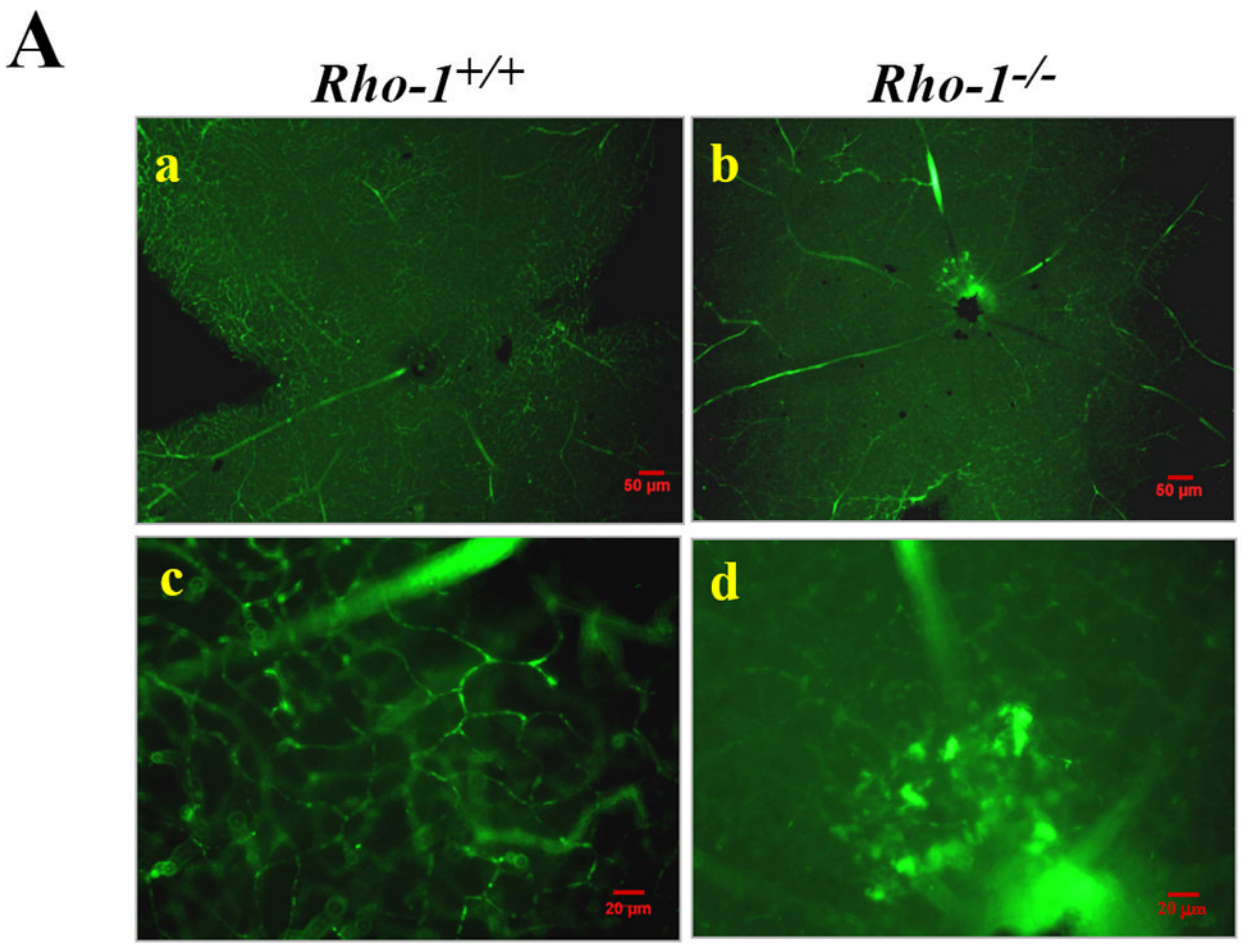

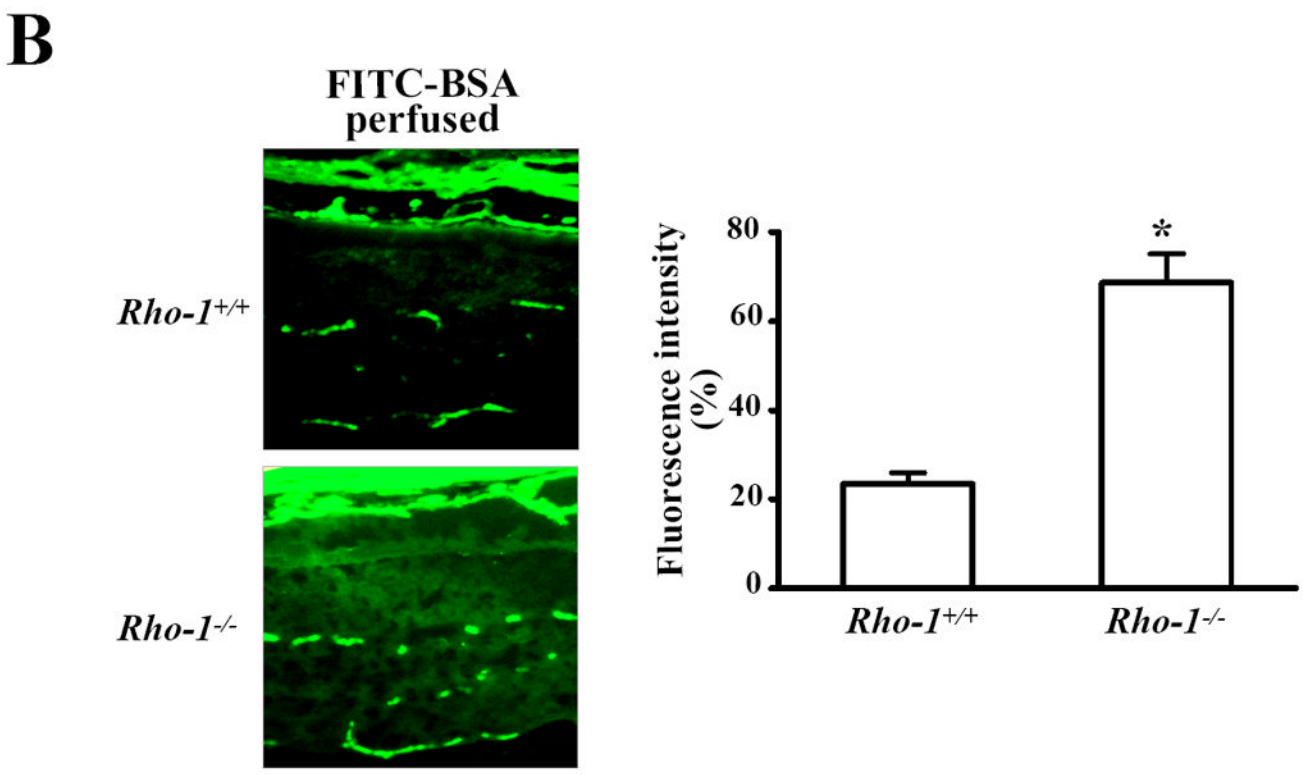

Figure 3.

Immunostaining and detection of FITC-albumin leakages in the retina of *rho-1*$^{-/-}$ knockout mice. **(A)** Detection of retinal vascular leakages in flat- and whole-mounted mouse retinal samples (upper panels). Enlarged areas were demonstrated for clear structures of the vasculature and vascular leakages (lower panels). The retina was cut and flat-mounted on a gelatin-coated slide. The vasculature was then examined under a fluorescent microscope. **(B)** Detection of retinal vascular leakages in retinal slides of *rho-1*$^{-/-}$ mice. Vascular leakages were detected under a *Nikon* fluorescent microscope (upper-panel). Fluorescent densities obtained from 5 eye sections from each eyeball were counted and analyzed (lower panel). Fluorescent intensities were scanned in the same area of the retina in each slide. Averages of 5 fields with the same dimension of areas were sampled and analyzed. Statistical significance was determined at the CI level of $p<0.05$, n=6).

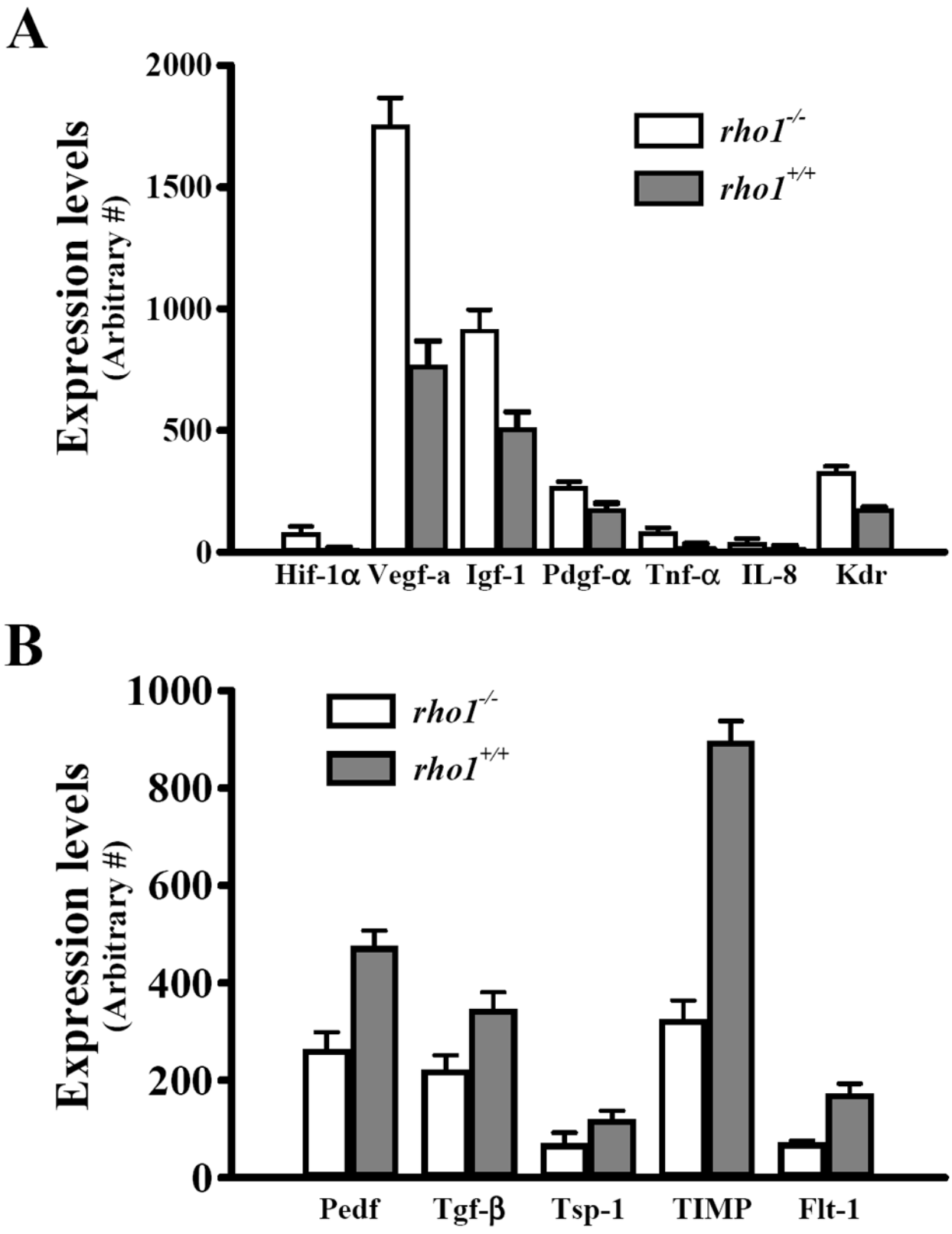

Figure 4.

Alterations of angiogenesis-associated gene expression profiles in the retina of *rho-1*$^{-/-}$ mice. **(A)** Up-regulation of angiogenic stimulators: VEGFα, IGF-1, PDGF, TNF-α, IL-8 and KDR. In addition, there was an increase in expression of HIF-1α. **(B)** Down-regulation of angiogenic inhibitors: PEDF, TGF-β, TSP-1, and FLT-1. In addition, there was a decrease in expression of metallo-proteinase inhibitor, TIMP. The expression profiles of the retina and RPE cells from *rho-1*$^{+/+}$ and *rho-1*$^{-/-}$ mice were compared. Statistical significance was determined at the CI level of $p<0.01$ (n = 6).

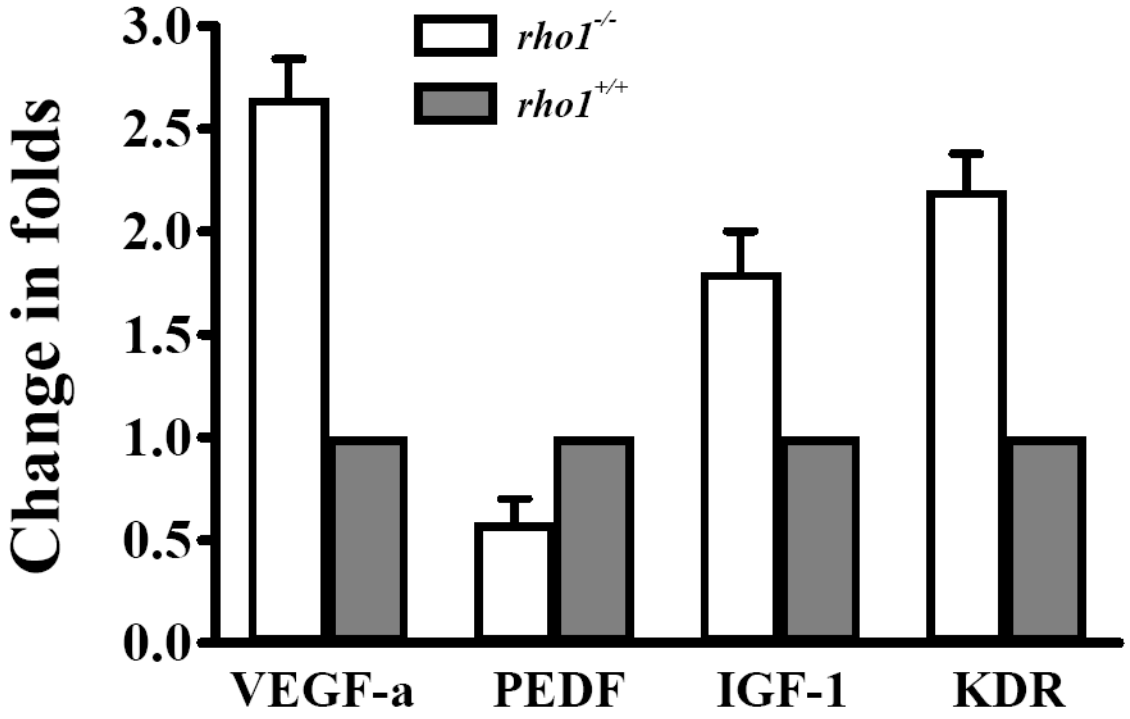

Figure 5.
Verification of gene expression modulations using SYBR-Green-I based real-time and quantitative PCR. The house-keeping gene GAPGH was used as normalizing standard. Gene expression fold-changes (*rho-1*$^{+/+}$ *vs rho-1*$^{-/-}$) were determined using the ΔΔCt method.